Published in final edited form as:
Clin Cancer Res. 2008 September 15; 14(18): 5900–5906. doi:10.1158/1078-0432.CCR-08-0846.

Gene Expression Profiling Reveals Similarities between the In vitro and In vivo Responses of Immune Effector Cells to Interferon-Alpha

Jason M. Zimmerer[1,2], **Gregory B. Lesinski**[2], **Amy S. Ruppert**[3], **Michael D. Radmacher**[3], **Carl Noble**[2], **Kari Kendra**[4], **Michael J. Walker**[4], and **William E. Carson III**[2,4]

[1] Integrated Biological Sciences Graduate Program, The Ohio State University Comprehensive Cancer Center, Columbus, OH 43210

[2] Human Cancer Genetics Program Department of Molecular Virology, Immunology, and Medical Genetics, The Ohio State University Comprehensive Cancer Center, Columbus, OH 43210

[3] Center for Biostastistics, The Ohio State University Comprehensive Cancer Center, Columbus, OH 43210

[4] Department of Surgery, The Ohio State University Comprehensive Cancer Center, Columbus, OH 43210

Abstract

Purpose—The precise molecular targets of interferon-alpha (IFN-α) therapy in the context of malignant melanoma are unknown but appear to involve STAT1 signal transduction within host immune effector cells. We hypothesized that the *in vitro* transcriptional response of patient PBMCs to IFN-α would be similar to the *in vivo* response to treatment with high-dose IFN-α.

Experimental Design—The gene expression profiles of peripheral blood mononuclear cells (PBMCs) and immune cell subsets treated *in vitro* with IFN-α were evaluated, as were PBMCs obtained from melanoma patients receiving adjuvant IFN-α.

Results—Twenty-seven genes were upregulated in PBMCs from normal donors following treatment with IFN-α *in vitro* for 18 hours (>2-fold, $p<0.001$). A subset of these genes (in addition to others) was significantly expressed in IFN-α treated T cells, NK cells, and monocytes. Analysis of gene expression within PBMCs from melanoma patients (n=13) receiving high-dose IFN-α-2b (20 MU/m^2 i.v.) revealed significant upregulation (>2-fold) of 21 genes ($p<0.001$). Also, the gene expression profile of *in vitro* IFN-α-stimulated patient PBMCs was similar to that of PBMCs obtained from the same patient following IFN-α therapy.

Conclusions—This report is the first to describe the transcriptional response of T cells, NK cells, and monocytes to IFN-α and to characterize the transcriptional profiles of PBMCs from melanoma patients undergoing IFN-α immunotherapy. In addition, it was determined that microarray analysis of patient PBMCs following *in vitro* stimulation with IFN-α may be a useful predictor of the *in vivo* response of immune cells to IFN-α immunotherapy.

Keywords

interferon-alpha; malignant melanoma; oligonucleotide microarray analysis; natural killer cell; T cell; monocyte

Address correspondence to: William E. Carson III, M.D., Department of Surgery, The Ohio State University, N924 Doan Hall, 410 West 10th Ave., Columbus, OH 43210, Phone: (614) 293-6306, Fax: (614) 293-3465, E-mail: william.carson@osumc.edu.

Introduction

Surgical treatment of early stage malignant melanoma is frequently curative. However, the therapeutic options for patients with metastatic disease are limited. IFN-α has been used both as an adjuvant following the surgical resection of high-risk lesions (lymph node metastases or primary tumor thickness >4 mm) and in the advanced disease setting. The IFN-α-receptor is expressed on melanoma tumor cells as well as on immune effectors and mediates many of its effects via activation of the Janus kinase (Jak)-signal transducers and activators of transcription (STAT) pathway. IFN-α exerts direct anti-proliferative, pro-apoptotic, and anti-angiogenic effects on melanoma cells in culture and has distinct immunostimulatory effects that vary according to the immune subset under study (1–4). Unfortunately, the precise molecular targets of exogenously administered IFN-α are unknown. As a result, it is not currently possible to identify patients who would have a high likelihood of responding to this treatment.

We have examined the role of the Jak-STAT signaling pathway in a murine model of malignant melanoma using STAT1-deficient mice and STAT1-deficient melanoma cell lines. It was found that loss of STAT1 signal transduction within the host abrogated the anti-tumor effects of IFN-α (5). In contrast, the survival benefits associated with IFN-α administration were maintained when normal (i.e., STAT1-competent) mice were challenged with a $STAT1^{-/-}$ murine melanoma cell line. We concluded that STAT1 signal transduction within the host, but not the tumor cell, was critical for mediating the anti-tumor effects of IFN-α. Further experiments by our group and others indicate that the immunostimulatory effects of IFN-α are an important component of its anti-tumor actions in mice (4,6–12). In fact, recent data have shown that the occurrence of autoimmune sequelae and the presence of tumor-infiltrating lymphocytes correlate with clinical response in patients receiving IFN-α (13,14). Together, these data suggest that the immunomodulatory actions of IFN-α are a critical component of its anti-tumor actions. However, a careful analysis of gene regulation within immune effector cells of cancer patients following IFN-α treatment has not been reported.

The gene expression profile of IFN-α stimulated peripheral blood mononuclear cells (PBMCs) and immune cell subsets (T cells, NK cells, and monocytes) was evaluated via microarray analysis as were the PBMCs from melanoma patients receiving high dose IFN-α-2b (20 MU/m^2 i.v.). We found that 27 genes were upregulated in the PBMCs of normal donors following treatment with IFN-α. A subset of these genes was also upregulated in T cells, NK cells, and monocytes. 21 genes were significantly induced in melanoma patient PBMCs *in vivo* following IFN-α therapy. The gene expression profile of PBMCs stimulated *in vitro* with IFN-α was similar to the gene expression profile of PBMCs obtained from the same patient following clinical administration of IFN-α. These results demonstrate that microarray analysis of patient PBMCs following *in vitro* stimulation with IFN-α may be a useful predictor of the biological response of patient PBMCs to IFN-α immunotherapy *in vivo*.

Materials and Methods

Reagents

Recombinant human (hu) IFN-α-2b (specific activity of 2×10^8 IU/mg) was purchased from Schering-Plough, Inc. (Kenilworth, NJ).

Isolation of Immune Subsets

For *in vitro* assays requiring total PBMCs or immune subsets, source leukocytes were obtained from healthy adult donors (American Red Cross, Columbus, OH). PBMCs were isolated by Ficoll-Paque Plus (Amersham Pharmacia Biotech, Uppsala, Sweden) density gradient

centrifugation as previously described (15). Lymphocytes were enriched for individual cell populations ($CD3^+$, $CD56^+$, and $CD14^+$ cells) by negative selection using RosetteSep reagents (Stem Cell Technologies, Vancouver, British Columbia). Following isolation, the purity of enriched cell populations was typically on the order of 95 – 99% as determined by flow cytometry (data not shown). Purified cells were then cultured in RPMI-1640 media supplemented with 10% human AB serum (Pel-Freez Clinical Systems, Brown Deer, WI) at 37°C with 5% CO_2 and stimulated with either 10^4 U/ml IFN-α-2b or PBS for 18 hours. Previous studies indicate that this dose of IFN-α approximates the levels seen following i.v. administration of IFN-α-2b (16). Following incubation, cells were harvested by centrifugation, resuspended in TRIzol reagent (Invitrogen), and processed for RNA extraction.

Patients and Blood Samples

Peripheral blood was obtained from melanoma patients (6 females, 7 males) immediately prior to, and one-hour following intravenous (i.v.) administration of high dose IFN-α-2b (20×10^6 IU/m^2). All samples were obtained at The Ohio State University following informed consent under an IRB-approved protocol (OSU 99H0348). PBMCs were isolated from peripheral blood (8 mL) via density gradient centrifugation with Ficoll-Paque Plus and immediately stored in TRIzol reagent (Invitrogen) at −80°C.

cRNA Preparation and Array Hybridization

Probe sets from U133 Plus 2.0 (Table 1) or U133A Arrays (Tables 2 and Supplemental Data Table 1; Affymetrix, Santa Clara, CA), which query approximately 47,000 or 22,000 human transcripts, respectively, were used in these analyses. U133 Plus 2.0 Arrays were also used for Table 3. The cRNA was synthesized as suggested by Affymetrix. Following lysis of cells in TRIzol (Invitrogen), mRNA was prepared by RNeasy purification (Qiagen, Valencia, CA). Double stranded cDNA was generated from 8 μg of total RNA using the Superscript Choice System according to the manufacturer's instructions (Invitrogen). Biotinylated cRNA was generated by *in vitro* transcription using the Bio Array High Yield RNA Transcript Labeling System (Enzo Life Sciences Inc., Farmingdale, NY). The cRNA was purified using the RNeasy RNA purification kit. cRNA was fragmented according to the Affymetrix protocol and the biotinylated cRNA was hybridized to U133A microarrays (17).

Data Analysis

Raw data were collected with a confocal laser scanner (Hewlett Packard, Palo Alto, CA) and probe level data were analyzed using dChip software (18). Invariant-set normalization was performed, and only perfect match probes were used in computing the model-based expression indices (MBEIs). "Array outliers," identified by dChip at the probe-set level, were set to missing. The $\log_2$(MBEIs) were then calculated and exported to BRB-ArrayTools software for further analysis. For each analysis, probe sets receiving an Affymetrix "Absent" call for more than 50% of the specimens were filtered. Paired t-tests were used in evaluating whether there was a difference in gene expression before and after treatment with IFN-α. All tests were two-sided and conducted at a nominal significance level of 0.001. In the non-screening analyses, testing for differential expression within a specific set of previously identified genes, the alpha level was set to 0.05 and *p*-values were adjusted using Holm's method to account for the multiple testing.

Real Time PCR

Gene expression estimates from the microarray experiments were validated by Real Time PCR for selected genes. Following TRIzol extraction and RNeasy purification for microarray analyses, 2 μg of total RNA was reverse transcribed and the resulting cDNA was used as a template to measure gene expression by Real Time PCR using pre-designed primer/probe sets

(Assays On Demand; Applied Biosystems, Foster City, CA) and 2X Taqman Universal PCR Master Mix (Applied Biosystems) according to the manufacturer's recommendations as previously described (19). Pre-designed primer/probe sets for human β-actin were used as an internal control in each reaction well (Applied Biosystems). Real Time PCR reactions were performed in triplicate in a capped 96-well optical plate. Real Time PCR data were analyzed using the ABI PRISM® 7900 Sequence Detection System (Applied Biosystems).

Results

Early transcriptional response of IFN-α-stimulated PBMCs from normal donors

In order to detect the genes that were induced immediately following IFN-α-stimulation, the gene expression profile of normal PBMCs (n=3) following a 1-hour *in vitro* treatment with IFN-α (10^4 U/mL) was evaluated (Table 1). This analysis showed that 22 genes were significantly upregulated more than 2-fold in response to treatment ($p<0.001$). The expression profile was characterized by the induction of genes encoding antiviral/immune response proteins (IFIH1, IFIT1, IFIT3, GBP1), chemo-attractants (CXCL10, CCL8), cytokines (IL-6), and other species, such as SOCS2 (an inhibitor of growth hormone signaling) and CASP4 (caspase 4, executor of cell death in response to endoplasmic reticulum stress). Real Time PCR was employed to validate the expression profiles of three representative genes (CXCL10, CCL8, IFIT1; Fig. 1).

Late transcriptional response of IFN-α-stimulated PBMCs from normal donors

Cell-to-cell interactions and autocrine cytokine stimulation likely influence the transcriptional profile of IFN-α-stimulated PBMCs Thus, the gene expression profile of normal PBMCs (n=3) following an 18 hour *in vitro* treatment with IFN-α (10^4 U/mL) was evaluated (Supplemental Data Table 1A) (20, 21). This analysis revealed that 27 genes were significantly upregulated more than 2-fold at this time point ($p<0.001$). The expression profile was characterized by the induction of genes encoding antiviral/immune response proteins (IFI16, IFI44), regulators of transcription (IRF2, SP110), T cell activation markers (LY6E), and other species such as CD38, USP18, and MT1H (Supplemental Data Table 1A). However, transcriptional regulation of the genes SPTLC2 (sphingolipid biosynthesis), N4BP1 (unknown function), and BLVRA (electron transport) by IFN-α has not been previously reported. These data were validated by measuring the expression of several notable genes expressed in PBMCs (IFIT2, ISG20, LY6E) by Real Time PCR (Supplemental Data Figure 1A).

Late transcriptional response of IFN-α-stimulated T cells, natural killer cells, and monocytes from normal donors

Similar *in vitro* experiments were conducted in $CD3^+$ T cells, $CD56^+$ natural killer (NK) cells, and $CD14^+$ monocytes (n=3 donors for each subset). The expression of 28 genes was significantly modulated more than 2-fold in the T cell compartment after IFN-α-2b stimulation (27 upregulated and 1 down-regulated, $p<0.001$; Supplemental Data Table 1B). These genes function in multiple processes including the regulation of apoptosis (TNFSF10), antigen binding (LAG3, MICB), regulation of the NFκB signal cascade (LGASL9, MYD88), transcriptional regulation (PHF11, SP100), and the antiviral response (IFI44, OAS3). The expression of 32 genes was modulated more than 2-fold in the NK cell compartment in response to IFN-α-2b treatment (30 upregulated and 2 down-regulated, $p<0.001$; Supplemental Data Table 1C). Several of these genes function in transcriptional regulation (IRF7, PML), as interferon class cytokine receptors (CLRF2), in cell motility (MARCKS), metal ion binding (MT1F, MT1H,), and the antiviral response (IFI27, OAS1). Finally, the expression of 51 genes was significantly regulated more than 2-fold following IFN-α-2b treatment of monocytes (33 upregulated and 18 down-regulated, $p<0.001$; Supplemental Data Table 1D). Several of these genes function in regulating apoptosis (CUL1, TFNRSF5), cell motility (PECAM1), antiviral

responses (GBP1, LCP2), immune cell activation (CD69), and regulation of transcription (IRF1, STAT1).

These findings were validated by measuring the expression of several notable genes expressed in T cells (IFIT1, LAG3, OAS3), NK cells (IRF7, ISG20, MX2), and monocytes (CD69, ISG20, OASL) by Real Time PCR (Supplemental Data Figure 1B–D). Of note, the gene expression profile of whole PBMCs at 18 hours is not a composite of the gene expression profiles of the individual immune subsets; 14 of the 27 genes induced in IFN-treated PBMCs were also upregulated in purified T cells (n=4), NK cells (n=7), or monocytes (n=8). This finding implies that IFN-α stimulation of whole PBMCs may be characterized by unique cellular interactions that occur between its constituent subsets. The cell-specific gene expression profiles suggest that each immune cell subset may respond to IFN-α in a unique fashion.

Gene regulation in PBMCs from melanoma patients receiving high dose IFN-α therapy

In order to characterize the *in vivo* immune response to IFN-α, PBMCs were isolated from the peripheral venous blood of 7 melanoma patients immediately prior to and 1 hour following the administration of the first dose of i.v. IFN-α-2b (20 MU/m^2). These patients were receiving IFN-α as an adjuvant therapy following surgical resection of high-risk melanoma lesions (lymph node disease or tumor >4 mm in depth). Analysis of the gene expression pattern of patient PBMCs showed that 23 genes were significantly upregulated more than 2-fold over baseline values following IFN-α-2b therapy ($p<0.001$; Table 2, Group 1). Genes involved in antigen presentation (TAP1), cell adhesion (LGALS3BP), and known IFN-α-stimulated genes (IFI44, IFIT4, IFITM3, IRF7, ISG20, OASL) were among those induced 1 hour post-IFN-α therapy in patient PBMCs. This experiment was repeated using PBMCs that were obtained from a second group of melanoma patients (n=6). This analysis verified that 21 of the 23 original genes were significantly upregulated in response to high dose i.v. IFN-α-2b (adjusted $p<0.05$; Table 2, Group 2). The last two genes (GPR43 and SCO2) were still found to be upregulated in this second analysis, but not to a significant degree. Real Time PCR was employed to validate the expression profiles of three representative genes (IRF7, OASL, TAP1; Fig. 2).

Comparison of IFN-α gene regulation in PBMCs stimulated *in vitro* with IFN-α to that of PBMCs obtained from the same donor before and after IFN-α therapy

We hypothesized that *in vitro* gene expression data might be used to predict the *in vivo* response of patient PBMCs to IFN-α. We therefore investigated the relationship between microarray results generated using PBMCs stimulated *in vitro* with IFN-α and those that were generated utilizing PBMCs obtained from the same patients pre- and post-IFN-α therapy. PBMCs were isolated from the peripheral venous blood of patients (n=6) immediately prior to and 1 hour following i.v. administration of IFN-α-2b (20 MU/m^2) and evaluated by microarray analysis for the expression of the 21 genes that we had previously confirmed as being regulated by IFN-α *in vivo* (Table 2). In addition, aliquots of the PBMCs collected prior to IFN-α therapy were treated *in vitro* with PBS or IFN-α (10^4 U/mL for 1 hour) and these were similarly evaluated by microarray analysis. As predicted, the vast majority of these genes (20 of 21, or 95.2%) were significantly induced over resting levels and were induced to a similar degree regardless of whether gene expression was occurring *in vitro* or *in vivo* (i.e., the ratio of *in vitro* to *in vivo* induction was less than 2-fold for these 20 genes) (Table 3). For example, in these six patients, IFIT3 was induced by an average of 36.4-fold *in vitro* and by an average of 33.4-fold *in vivo*. Additionally, the majority of these genes (67%) did not show a significant difference in gene expression between the *in vitro* or *in vivo* samples (adjusted $p>0.05$). Thus, the *in vitro* transcriptional response of patient PBMCs to IFN-α appeared largely similar to the *in vivo* transcriptional response of PBMCs to treatment with high dose IFN-α. This result

demonstrates that microarray analysis of patient PBMCs following *in vitro* stimulation with IFN-α may be a useful predictor of the biological response of patient PBMCs to IFN-α immunotherapy *in vivo*.

Discussion

We set out to characterize the gene expression profiles of PBMCs and immune subsets in response to IFN-α and to determine whether *in vitro* gene expression profiling of the immune response to IFN-α could predict the *in vivo* response of immune effector cells to adjuvant IFN-α. In determining the transcriptional response of immune cells to IFN-α using microarray analysis, we found the following: 1) immune cell subsets exhibited distinct IFN-α-induced gene expression profiles that were not entirely reflective of the overall PBMC profile and 2) the gene expression profile of *in vitro* IFN-α-stimulated PBMCs was similar to the PBMC gene expression profile following IFN-α administration within the same patient. These data suggest that microarray analysis of PBMCs *in vitro* may be a useful predictor of the biological response of patient PBMCs to IFN-α immunotherapy *in vivo*.

Microarray analysis of PBMCs from normal donors identified 22 genes that were upregulated greater than 2-fold in response to *in vitro* IFN-α treatment at the 1 hour time point and 27 genes at the 18 hour time point ($p<0.001$). Of note, there was no overlap in the genes that were induced at these two time points. This result suggested that the IFN-α-induced gene expression profile of human immune cells may vary according to the duration of the cytokine stimulus. In further support of this notion, Ji *et al*. reported only a modest overlap of the 516 genes induced at 3 or 6 hours following *in vitro* treatment of PBMCs with 200 U/ml of IFN-α (22). This group's use of cells from patients with chronic hepatitis C is an important difference from the current study, since the presence of this chronic viral infection likely enhanced the expression of multiple genes with anti-viral effects. A comparison of our *in vitro* microarray analysis results with this previous study revealed overlap for only a few genes (i.e., IFIT1, IFI-16, IFIT2). This small overlap in genes may be due to differences in statistical methods, time points examined, IFN-α dosages, and the presence of varying degrees of viral load.

An analysis of immune cell subsets showed that 14 of the 27 genes that were induced in IFN-α-stimulated PBMCs at 18 hours (OAS2, OASL, HERC5, ISG20, IFI44, LIR7, LGP2, MT1H, MT2A, N4BP1, PLSCR1, USP18, TREX1, ZCCHC2) were also upregulated in T cells, NK cells or monocytes (as denoted in Supplemental Data Table 1B–D by a "**"). This implied that the functional responses of these compartments to exogenous IFN-α were vigorous, yet distinct. A comparison of these results with those of other investigators obtained using virally-infected cells treated with IFN-α (e.g., endothelial, hepatoblastoma, and keratinocyte cell lines) revealed only minor similarities and underscored the tissue specificity of IFN-α-induced signal transduction and gene regulation (23–27). Of note, the gene expression profile of IFN-α stimulated monocytes was similar to data from a previous report of IFN-stimulated mononuclear phagocytes that had been pretreated with lipopolysaccharide *in vitro* (28). "Signature" genes induced by IFN-α in both reports included GBP1, ISG20, MX1, STAT1, and OAS3 among others. The IFN-response of the monocyte compartment was also unique in that several dozen genes were significantly down-regulated following IFN-α treatment. This implies that there is significant basal expression of a set of ISGs in monocytes.

This is the first study to employ microarray techniques to analyze the transcriptional profile of circulating PBMCs obtained from cancer patients immediately following IFN-α immunotherapy (29). We were somewhat surprised at the relatively low number of genes that were significantly induced in response to this high dose of cytokine. It will be interesting to see if these same levels of gene induction are maintained in response to subsequent doses of IFN-α. The gene expression profile of patient PBMCs treated *in vitro* with IFN-α closely

matched the expression profile of PBMCs obtained after IFN-α administration in these same patients. The fact that similar results were obtained in two separate cohorts of patients supports the validity of our conclusions. Interestingly, a comparison of the *in vitro* IFN-α-induced gene expression pattern of PBMCs from normal donors (Table 1) with the *in vitro* response of PBMCs from melanoma patients (Table 3 and data not shown) revealed important similarities; 18 of the 22 genes upregulated in normal donor PBMCs were also upregulated by more than 2-fold in melanoma patient PBMCs following *in vitro* stimulation with IFN-α. Only CCL10, CD274, LOC341720, and SAMD9L were not induced by more than 2-fold in melanoma patient PBMCs following *in vitro* stimulation with IFN-α. Greater differences in gene expression may be identified in patients with metastatic melanoma. These findings support the use of microarray analysis of *in vitro* stimulated immune cells to predict the individual patient gene response to cytokine therapy. This may allow for improved selection of patients who would benefit from IFN-α administration.

We have identified several IFN-α-regulated genes that could be important mediators of the anti-tumor effects of IFN-α. These genes include CXCL9, CXCL10, HERC5, USP18, and TAP1. IFN-α stimulates the production of CXCL10 and CXCL9 by monocytes and these two factors exert a strong chemotactic effect on T cells (Supplemental Data Table 1) (30–34). HERC5 and USP18 are involved in the ubiquitin-mediated catabolism of antigenic proteins and their induction by IFN-α could lead to enhanced presentation of antigenic peptides by antigen presenting cells (35). IFN-α is also able to enhance antigen presentation through its ability to increase the expression of TAP1, a key regulator of antigen transport within the endoplasmic reticulum (36, 37). The upregulation of these genes suggests a potential mechanism of IFN-α's ability to facilitate an adaptive $CD8^+$ T cell immune response (38).

The present study demonstrated that the transcriptional profile of IFN-α-stimulated immune cells can be affected by multiple factors including duration of stimulation, cell type, and the method of exposure to cytokine (i.e., *in vitro* stimulation versus *in vivo* administration). Importantly, we found that *in vitro* analysis of IFN-α-stimulated PBMCs may be predictive of the *in vivo* expression profile following IFN-α immunotherapy. Further investigation of this finding and its relation to the clinical situation is warranted.

Supplementary Material

Refer to Web version on PubMed Central for supplementary material.

Acknowledgments

The authors thank The Ohio State University Comprehensive Cancer Center (CCC) Microarray Core Facility for performing cRNA hybridization and the raw data collection. We also thank The Ohio State University CCC Real Time Core Facility for assisting in the operation of the ABI PRISM® 7900 Sequence Detection System. Some statistical analyses were performed using BRB-ArrayTools version 3.22 developed by Dr. Richard Simon and Amy Peng Lam.

Support: This work was supported in part by a Career Development Award from the Melanoma Research Foundation (to G.B.L.), The Valvano Foundation for Cancer Research (to G.B.L), and National Institutes of Health (NIH) Grants K24 CA93670, P30-CA16058, and P01 CA95426-01A1 (all to W.E.C.).

References

1. Maellaro E, Pacenti L, Del Bello B, et al. Different effects of interferon-alpha on melanoma cell lines: a study on telomerase reverse transcriptase, telomerase activity and apoptosis. Br J Dermatol 2003;148:1115–1124. [PubMed: 12828737]
2. Bauer JA, Morrison BH, Grane RW, et al. IFN-alpha2b and thalidomide synergistically inhibit tumor-induced angiogenesis. J Interferon Cytokine Res 2003;23:3–10. [PubMed: 12639293]

3. Garbe C, Krasagakis K, Zouboulis CC, et al. Antitumor activities of interferon alpha, beta, and gamma and their combinations on human melanoma cells in vitro: changes of proliferation, melanin synthesis, and immunophenotype. J Invest Dermatol 1990;95:231S–237S. [PubMed: 2124247]
4. Belardelli F, Ferrantini M, Proietti E, Kirkwood JM. Interferon-alpha in tumor immunity and immunotherapy. Cytokine Growth Factor Rev 2002;13:119–134. [PubMed: 11900988]
5. Lesinski GB, Anghelina M, Zimmerer J, et al. The antitumor effects of IFN-alpha are abrogated in a STAT1-deficient mouse. J Clin Invest 2003;112:170–180. [PubMed: 12865406]
6. Belardelli F, Gresser I, Maury C, Maunoury MT. Antitumor effects of interferon in mice injected with interferon-sensitive and interferon-resistant Friend leukemia cells. I Int J Cancer 1982;30:813–820.
7. Belardelli F, Gresser I, Maury C, Maunoury MT. Antitumor effects of interferon in mice injected with interferon-sensitive and interferon-resistant Friend leukemia cells. II. Role of host mechanisms. Int J Cancer 1982;30:821–825. [PubMed: 6186615]
8. Gresser I, Maury C, Carnaud C, et al. Anti-tumor effects of interferon in mice injected with interferon-sensitive and interferon-resistant Friend erythroleukemia cells. VIII. Role of the immune system in the inhibition of visceral metastases. Int J Cancer 1990;46:468–474. [PubMed: 2394514]
9. Gresser I, Kaido T, Maury C, et al. Interaction of IFN alpha/beta with host cells essential to the early inhibition of Friend erythroleukemia visceral metastases in mice. Int J Cancer 1994;57:604–611. [PubMed: 8181864]
10. Fallarino F, Gajewski TF. Cutting edge: differentiation of antitumor CTL in vivo requires host expression of Stat1. J Immunol 1999;163:4109–4113. [PubMed: 10510345]
11. Lesinski GB, Valentino D, Hade EM, et al. Expression of STAT1 and STAT2 in malignant melanoma does not correlate with response to interferon-alpha adjuvant therapy. Cancer Immunol Immunother. 2005
12. Zimmerer JM, Lesinski GB, Kondadasula SV, Karpa V, Lehman A, RayChaudhury, Becknell B, Carson WE. IFN-alpha-Induced signal transduction, gene expression, and anti-tumor activity of immune effector cells are negatively regulated by suppressors of cytokine signaling proteins. J Immunol 2007;178:4832–4845. [PubMed: 17404264]
13. Koon H, Atkins M. Autoimmunity and immunotherapy for cancer. N Engl J Med 2006;354:758–760. [PubMed: 16481646]
14. Moschos SJ, Edington HD, Land SR, et al. Neoadjuvant treatment of regional stage IIIB melanoma with high-dose interferon alfa-2b induces objective tumor regression in association with modulation of tumor infiltrating host cellular immune responses. J Clin Oncol 2006;24:3164–3171. [PubMed: 16809739]
15. Parihar R, Dierksheide J, Hu Y, Carson WE. IL-12 enhances the natural killer cell cytokine response to Ab-coated tumor cells. J Clin Invest 2002;110:983–992. [PubMed: 12370276]
16. Islam M, Frye RF, Richards TJ, et al. Differential effect of IFNalpha-2b on the cytochrome P450 enzyme system: a potential basis of IFN toxicity and its modulation by other drugs. Clin Cancer Res 2002;8:2480–2487. [PubMed: 12171873]
17. Moschella F, Bisikirska B, Maffei A, et al. Gene expression profiling and functional activity of human dendritic cells induced with IFN-alpha-2b: implications for cancer immunotherapy. Clin Cancer Res 2003;9:2022–2031. [PubMed: 12796364]
18. Li C, Wong WH. The analysis of gene expression data: methods and software. DNA-Chip Analyzer (dChip). 2003
19. Tokuhiro S, Yamada R, Chang X, et al. An intronic SNP in a RUNX1 binding site of SLC22A4, encoding an organic cation transporter, is associated with rheumatoid arthritis. Nat Genet 2003;35:341–348. [PubMed: 14608356]
20. Honda K, Yanai H, Negishi H, et al. IRF-7 is the master regulator of type-I interferon-dependent immune responses. Nature 2005;434:772–777. [PubMed: 15800576]
21. Takaoka A, Yanai H, Kondo S, et al. Integral role of IRF-5 in the gene induction programme activated by Toll-like receptors. Nature 2005;434:243–249. [PubMed: 15665823]
22. Ji X, Cheung R, Cooper S, et al. Interferon alfa regulated gene expression in patients initiating interferon treatment for chronic hepatitis C. Hepatology 2003;37:610–621. [PubMed: 12601359]

23. Wang X, Yuan ZH, Zheng LJ, et al. Gene expression profiles in an hepatitis B virus transfected hepatoblastoma cell line and differentially regulated gene expression by interferon-alpha. World J Gastroenterol 2004;10:1740–1745. [PubMed: 15188497]
24. Geiss GK, Carter VS, He Y, et al. Gene expression profiling of the cellular transcriptional network regulated by alpha/beta interferon and its partial attenuation by the hepatitis C virus nonstructural 5A protein. J Virol 2003;77:6367–6375. [PubMed: 12743294]
25. Zhu H, Zhao H, Collins CD, et al. Gene expression associated with interferon alfa antiviral activity in an HCV replicon cell line. Hepatology 2003;37:1180–1188. [PubMed: 12717400]
26. Chang YE, Laimins LA. Microarray analysis identifies interferon-inducible genes and Stat-1 as major transcriptional targets of human papillomavirus type 31. J Virol 2000;74:4174–4182. [PubMed: 10756030]
27. Gomez D, Reich NC. Stimulation of primary human endothelial cell proliferation by IFN. J Immunol 2003;170:5373–5381. [PubMed: 12759411]
28. Stroncek DF, Basil C, Nagorsen D, et al. Delayed polarization of mononuclear phagocyte transcriptional program by type I interferon isoforms. J Transl Med 2005;3:24. [PubMed: 15953390]
29. Zimmerer, JM.; Lesinski, GB.; Kornacker, K.; Shen, L.; Liyanarachichi, S.; Durbin, J.; Kendra, K.; Walker, M.; Carson, WE. Gene expression profiling of the response to interferon-alpha immunotherapy. American Association for Cancer Research Annual Meeting; Orlando, FL. 2003. Abstract #4679
30. Luster AD, Unkeless JC, Ravetch JV. Gamma-interferon transcriptionally regulates an early-response gene containing homology to platelet proteins. Nature 1985;315:672–676. [PubMed: 3925348]
31. Lee HH, Farber JM. Localization of the gene for the human MIG cytokine on chromosome 4q21 adjacent to INP10 reveals a chemokine “mini-cluster”. Cytogenet Cell Genet 1996;74:255–258. [PubMed: 8976378]
32. Farber JM. Mig and IP-10: CXC chemokines that target lymphocytes. J Leukoc Biol 1997;61:246–257. [PubMed: 9060447]
33. Dufour JH, Dziejman M, Liu MT, et al. IFN-gamma-inducible protein 10 (IP-10; CXCL10)-deficient mice reveal a role for IP-10 in effector T cell generation and trafficking. J Immunol 2002;168:3195–3204. [PubMed: 11907072]
34. Angiolillo AL, Sgadari C, Taub DD, et al. Human interferon-inducible protein 10 is a potent inhibitor of angiogenesis in vivo. J Exp Med 1995;182:155–162. [PubMed: 7540647]
35. Wang J, Maldonado MA. The ubiquitin-proteasome system and its role in inflammatory and autoimmune diseases. Cell Mol Immunol 2006;3:255–261. [PubMed: 16978533]
36. Longman RS, Braun D, Pellegrini S, et al. Dendritic-cell maturation alters intracellular signaling networks, enabling differential effects of IFN-alpha/beta on antigen cross-presentation. Blood 2007;109:1113–1122. [PubMed: 17018853]
37. Marusina K, Reid G, Gabathuler R, Jefferies W, Monaco JJ. Novel peptide-binding proteins and peptide transport in normal and TAP-deficient microsomes. Biochemistry 1997;36:856–863. [PubMed: 9020784]
38. Lapenta C, Santini SM, Spada M, et al. IFN-alpha-conditioned dendritic cells are highly efficient in inducing cross-priming CD8(+) T cells against exogenous viral antigens. Eur J Immunol 2006;36:2046–2060. [PubMed: 16856207]

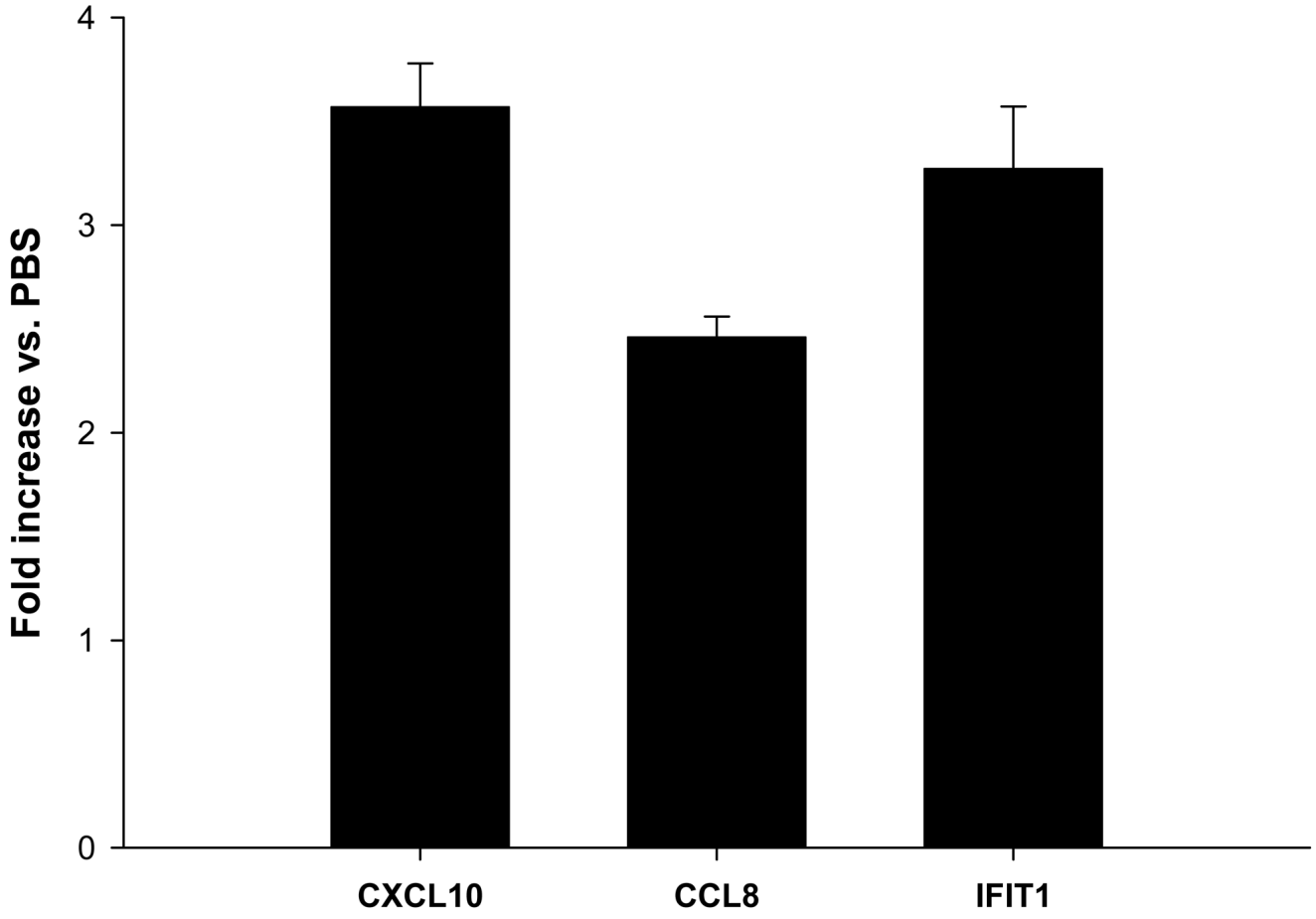

Figure 1. Real Time PCR analysis of select genes identified by microarray analysis of normal PBMCs following 1 hour *in vitro* IFN-α stimulation

Real Time PCR was used to validate the expression of genes in PBMCs (CXCL10, CCL8, IFIT1). Data were expressed as the mean fold increase relative to baseline levels (PBS treatment). All real time PCR data were normalized to the level of β-actin mRNA. Error bars denote the standard deviations of triplicate experiments.

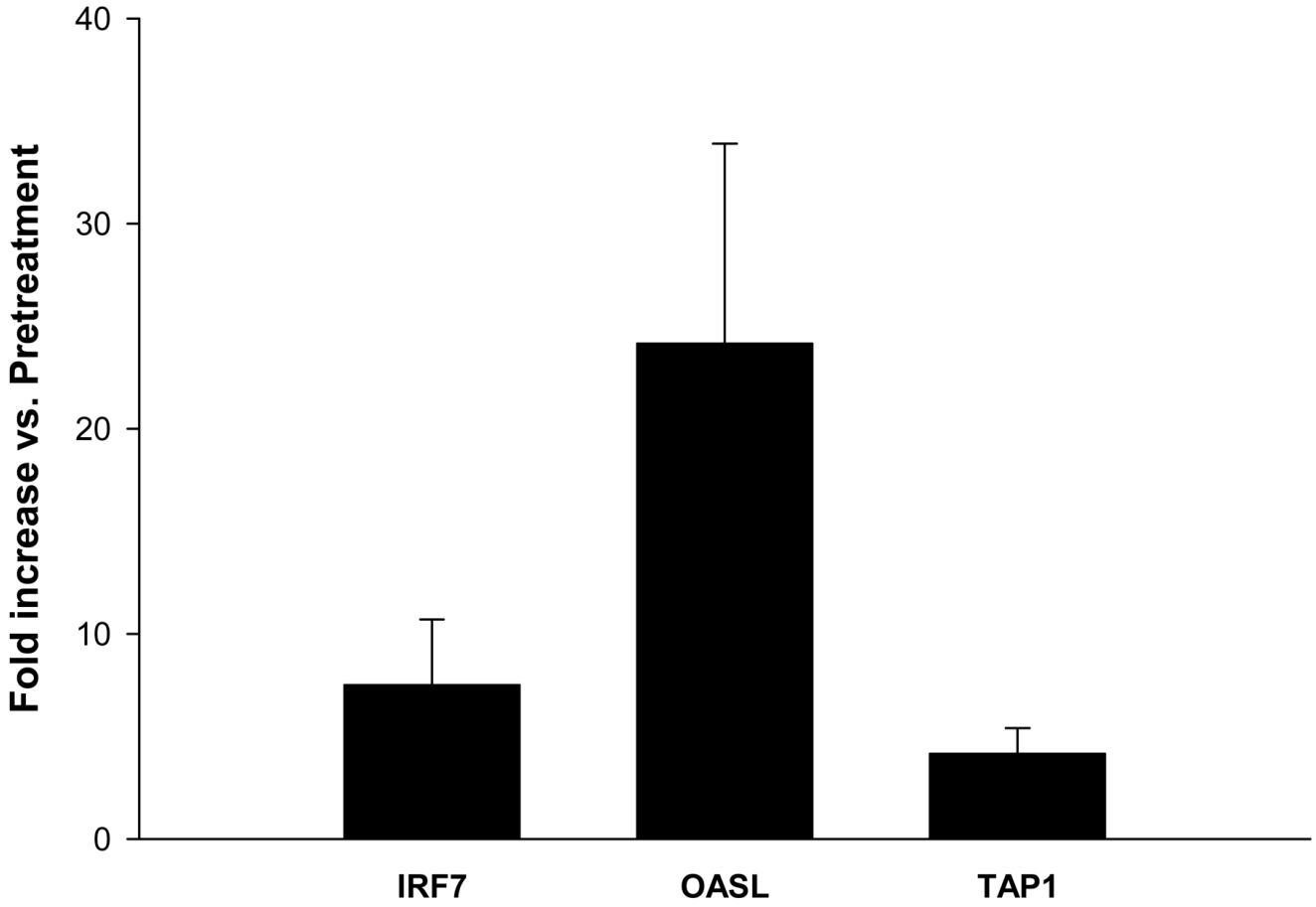

Figure 2. Real Time PCR analysis of select genes identified by microarray analysis of PBMCs from melanoma patients receiving IFN-α

Real Time PCR was used to validate the expression of representative genes (IRF7, OASL, TAP1). Data were expressed as the mean fold increase relative to baseline levels (pre-treatment). All real time PCR data were normalized to the level of β-actin mRNA. Patient gene expression estimates were pooled and error bars denote the standard deviations of 7 melanoma patients.

Table 1

Gene Regulation in PBMCs from normal donors following 1hr IFN-α treatment in vitro

Gene	Function	Fold Change Post vs Pre- treatment
Chemokine (C-X-C motif) ligand 10*(CXCL10)*	Chemotaxis, stimulates NK cells and monocytes	176.1
Chemokine (C-C motif) ligand 8*(CCL8)*	Chemotaxis	122.3
Interferon-induced protein with tetratricopeptide repeats 1 *(IFIT1)*	Immune response	117.2
Interferon-induced protein with tetratricopeptide repeats 3 *(IFIT3)*	Immune response	62.2
Sterile alpha motif domain containing 9-like *(SAMD9L)*	Unknown	44.3
LOC341720	Unknown	24.6
Cholesterol 25-hydroxylase *(CH25H)*	Catalytic activity	21.3
Guanylate binding protein 1*(GBP1)*	Immune response	13.9
CD274 antigen *(CD274)*	Immune response, cell proliferation	13.7
Nuclear receptor coactivator 7*(NCOA7)*	Transcriptional regulation, nucleic acid metabolism	8.5
FLJ20968	Unknown	7.3
Interferon induced with helicase C domain 1 *(IFIH1)*	Regulation of apoptosis, regulation of translation	5.6
FLJ11000	Unknown	4.5
FLJ10159	Unknown	4.4
EST sequence	Unknown	4.3
Caspase 4 *(CASP4)*	Induction of apoptosis	3.9
Interleukin 6 *(IL6)*	B cell and T cell differentiation	3.6
EST sequence	Unknown	3.6
Suppressor of cytokine signaling 2*(SOCS2)*	Inhibition of Jak/STAT signaling	2.8
EST sequence	Unknown	2.5
T-cell activation GTPase activating protein *(TAGAP)*	GTPase activator	2.4
ADP-ribosylation factor-like 8*(ARL8)*	GTPase	2.1

Genes had a probe set differentially expressed by more than 2-fold ($p < 0.001$).

Table 2

Gene Regulation in PBMCs Obtained from Melanoma Patients 1hr Following i.v. Administration of IFN-α-2B at 20 MU/m^2

Gene	Function	1st Group, Fold Change Post vs Pre-treatment*	2nd Group, Fold Change Post vs Pre-treatment	2nd Group, Adjusted P
Interferon-induced protein with tetratricopeptide repeats 3 *(IFIT3)*	Antiviral Response	12.0	33.4	<0.001
Ubiquitin specific protease 18 *(USP18)*	Protein Catabolism	5.8	42.8	<0.001
Interferon-induced protein 44 *(IFI44)*	Invasive growth, antiviral response	5.5	9.5	<0.001
2′-5′-oligoadenylate synthetase-like *(OASL)*	Double-stranded RNA binding, DNA binding	5.0†	16.2†	<0.001
Interferon regulatory factor 7 *(IRF7)*	Transcription factor, antiviral response	3.7	5.2	<0.001
Zinc finger, CCHC domain containing 2 *(ZCCHC2)*	Nucleic acidic binding	3.2	4.9	<0.001
EST sequence	Unknown	3.0	6.7	<0.001
Tumor necrosis factor receptor superfamily, member 6 *(TNFRSF6)*	Apoptosis	3.0	4.9	<0.001
Metallothionein 1H *(MT1H)*	Metal ion binding	2.8	3.2	<0.001
Interferon stimulated gene 20kDa *(ISG20)*	Cell proliferation, exonuclease activity	2.7†	4.5†	<0.001
Zinc finger CCCH type domain containing 1 *(ZC3HDC1)*	Nucleic acidic binding	2.5	5.1	<0.001
Three prime repair exonuclease 1 *(TREX1)*	DNA repair	2.4	4.0	<0.001
Transporter 1, ATP-binding cassette, sub-family B *(TAP1)*	Antigen presentation	2.4	3.6	<0.001
Hypothetical protein FLJ11286	Unknown	2.4	3.5	<0.001
Promyelocytic leukemia *(PML)*	Transcription factor, cell growth	2.2	5.4	<0.001
GTP cyclohydrolase 1 *(GCH1)*	Neurotransmitter	2.6	2.5	0.001
Interferon induced transmembrane protein 3 *(IFITM3)*	Immune response	2.3	1.8	0.001
Metallothionein 1E *(MT1E)*	Metal ion binding	2.1	2.8	0.001
Lectin, galactoside-binding, soluble, 3 binding protein *(LGALS3BP)*	Cell adhesion, scavenger receptor	2.1	2.0	0.002
Serine palmitoyltransferase, long chain base subunit 2 *(SPTLC2)*	Acyltransferase	2.5	2.3	0.006
Nuclear factor, interleukin 3 regulated *(NFIL3)*	Cellular Survival	3.7	2.8	0.01
G protein-coupled receptor 43 *(GPR43)*	Rhodopsin-like receptor	2.3	2.7	0.17
SCO cytochrome oxidase deficient homolog 2 *(SCO2)*	Electron transport	2.1	1.2	0.27

*Genes were significantly upregulated by more than 2-fold ($p < 0.001$)

†Significant gene upregulation was observed in multiple probe sets. The displayed changes in expression are the average (geometric mean).

Table 3

Comparison of Gene Expression Profiles Following *In vitro* and *In vivo* Treatment of Patient PBMCs with IFN-α-2b

Probe set	Gene symbol	*In vitro*, Fold Change Post vs Pre-treatment	*In vivo*, Fold Change Post vs Pre-treatment	Ratio of *In vitro* Fold-change to *In vivo* Fold-Change (Average, Range)	Adjusted P
203574_at	NFIL3	5.44	2.83	1.92, 1.45–2.66	0.014
205660_at 210797_s_at	OASL OASL	29.06 25.50	17.39 15.12	1.67, 1.50–2.28 1.69, 1.55–2.25*	0.009 0.007
204224_s_at	GCH1	3.09	2.50	1.24, 0.91–1.83	0.796
204747_at	IFIT3	36.43	33.42	1.09, 1.01–1.33	0.833
33304_at 204698_at	ISG20 ISG20	4.53 4.53	4.45 4.54	1.02, 0.86–1.15 1.00, 0.84–1.12*	1.000 1.000
208436_s_at	IRF7	5.09	5.16	0.99, 0.76–1.24	1.000
212859_x_at	MT1E	2.65	2.81	0.94, 0.75–1.19	1.000
202307_s_at	TAP1	3.43	3.65	0.94, 0.81–1.27	1.000
211012_s_at	PML	4.97	5.36	0.93, 0.62–1.49	1.000
206461_x_at	MT1H	2.91	3.17	0.92, 0.77–1.17	1.000
216565_x_at	LOC391020	1.58	1.76	0.90, 0.72–1.25	1.000
214453_s_at	IFI44	6.71	9.49	0.71, 0.62–1.03	0.093
200923_at	LGALS3BP	1.30	1.97	0.66, 0.53–1.09	0.129
219062_s_at	ZCCHC2	3.09	4.91	0.63, 0.44–1.04	0.187
215719_x_at	FAS	3.09	4.90	0.63, 0.52–0.76	0.014
205875_s_at	TREX1	2.53	4.00	0.63, 0.48–0.72	0.013
218543_s_at	PARP12	3.05	5.14	0.59, 0.44–0.95	0.078
219211_at	USP18	22.32	42.81	0.52, 0.35–0.87	0.050
53720_at	FLJ11286	1.81	3.52	0.52, 0.43–0.69	0.007
213294_at	EST sequence	3.43	6.70	0.51, 0.36–0.79	0.035
216202_s_at	SPTLC2	1.09	2.34	0.47, 0.37–0.64	0.008

* The geometric mean and range of OASL transcript = 1.68, 1.52–2.27, and ISG20 transcript = 1.01, 0.85–1.14.